

High temperature expansion for the Gaussian core model

Frank H. Stillinger

Bell Telephone Laboratories, Murray Hill, New Jersey 07974
(Received 10 January 1979)

Exact series coefficients through eighth order are reported for the high temperature expansion of the Gaussian core model free energy. Although this expansion has a vanishing radius of convergence it can be summed by a Borel integral transform. It is demonstrated that this Borel transform has an intimate connection to "crystallites" in the stable fluid phase which causes it to display a replica of the distribution function for large crystallites. This last observation permits implementation of a transform subtractive procedure which generates metastable extensions of fluid properties into the supercooled regime below the thermodynamic freezing temperature.

I. INTRODUCTION

In spite of many attempts, a comprehensive theory for the fluid-crystal transition has not yet been devised. A possible approach which seems to have received minimal attention thus far is the study of these transitions through high temperature expansions for the relevant partition functions. This paper is devoted to that approach, at least in an exploratory sense. The analysis presented here is restricted to the classical "Gaussian core model," since that is the case (among continuum systems, as distinct from lattice systems) for which the high temperature series can most conveniently be evaluated.

As a result of previous work several interesting properties have been established for the Gaussian core model. For example it has been proved that this model reduces to the classical rigid sphere model in a suitable low-temperature, low-density limit.¹ Furthermore in three dimensions it displays at least two different crystal structures.¹ Extensive computer simulation studies have also revealed unusual behavior once considered uniquely to belong to water, namely a fluid-phase density maximum and an increase in self-diffusion rate with increasing pressure.²

The formal series expansion for the free energy of the Gaussian core model is carried out in the following Sec. II, and exact series coefficients have been worked out through eighth order. Some numerical properties of these coefficients are explored in Sec. III. Because the series is a nonconvergent asymptotic series, the Borel transform is invoked in Sec. IV to facilitate analytical study of the phase transition; this transform will also facilitate comparison of present theoretical results with computer simulation studies. An important connection between crystallite distribution in the fluid and the Borel transform is presented in Sec. V. This in turn shows how to generate metastable extensions of fluid properties into the supercooled regime (Sec. VI). Section VII indicates possible areas for future study.

II. FORMAL SERIES DEVELOPMENT

Using suitably reduced units for length and energy, the N -molecule potential function Φ_N for the Gaussian core model has the following elementary form:

$$\Phi_N(\mathbf{r}_1 \cdots \mathbf{r}_N) = \sum_{i < j=1}^N \exp(-r_{ij}^2). \quad (2.1)$$

The corresponding canonical partition function is:

$$Z_N(\beta) = \frac{1}{\lambda^{DN} N!} \int_V d\mathbf{r}_1 \cdots \int_V d\mathbf{r}_N \exp(-\beta\Phi_N), \quad (2.2)$$

$$\beta = (k_B T)^{-1}, \quad \lambda = h(2\pi m k_B T)^{-1/2}.$$

Here D stands for the dimension of the system "volume" V , which each integral in Eq. (2.2) spans.

The Helmholtz free energy can be obtained directly from Z_N . For present purposes we need to focus attention on $f(\beta)$, the excess free energy per particle, which is given by:

$$\exp(-N\beta f) = \langle \exp(-\beta\Phi_N) \rangle. \quad (2.5)$$

The averaging operation indicated here is simply

$$\langle \exp(-\beta\Phi_N) \rangle = V^{-N} \int_V d\mathbf{r}_1 \cdots \int_V d\mathbf{r}_N \exp(-\beta\Phi_N). \quad (2.6)$$

It is elementary to show that this last quantity is analytic in β throughout the entire complex β plane (for finite N and V). Φ_N is always finite, so the integrand may be expanded in a power series; hence

$$\exp(-N\beta f) = \sum_{n=0}^{\infty} \frac{(-\beta)^n}{n!} \langle \Phi_N^n \rangle. \quad (2.7)$$

Taking logarithms in Eq. (2.7), the moment expansion is converted into a cumulant expansion:

$$N\beta f(\beta) = - \sum_{l=1}^{\infty} (-\beta)^l \Lambda_l. \quad (2.8)$$

The Λ_l are determined by the formula³

$$\Lambda_l = \sum'_{\{n_j\}} (-1)^{\sum n_j - 1} (\sum n_j - 1)! \prod_{j=1}^{\infty} \frac{\langle \Phi_N^{n_j} \rangle}{n_j! (j!)^{n_j}}, \quad (2.9)$$

where the primed summation includes all distinct sets (n_1, n_2, n_3, \dots) of nonnegative integers subject to the restriction

$$\sum_{j=1}^{\infty} j n_j = l. \quad (2.10)$$

Whereas moment series (2.7) converges everywhere in the complex β plane, cumulant series (2.8) will converge only up to the radius of the moment series zero nearest the origin.

By inserting the specific interaction (2.1) into the general cumulant formula (2.9) one easily finds the lowest order cumulants to be:

$$\Lambda_1 = \frac{N(N-1)}{2V^2} \int_V d\mathbf{r}_1 \int_V d\mathbf{r}_2 \exp(-r_{12}^2); \quad (2.11)$$

$$\Lambda_2 = \frac{N(N-1)}{4} \left\{ \frac{1}{V^2} \int_V d\mathbf{r}_1 \int_V d\mathbf{r}_2 \exp(-2r_{12}^2) - \left[\frac{1}{V^2} \int_V d\mathbf{r}_1 \int_V d\mathbf{r}_2 \exp(-r_{12}^2) \right]^2 \right\}. \quad (2.12)$$

Similar but more complex expressions are obtained in succeeding orders.

It would certainly be instructive to have evaluated cumulants to high order l for general N and V since this would clarify the way that the fluid–solid transition develops upon approaching the infinite system-size limit. However the advantageous simplifications offered by the Gaussian core model are realized only when integration limits are infinite, i. e., when V itself becomes infinite. Thus we are obliged to pass immediately to the infinite system size limit with $N/V = \rho$ held fixed. In this limit we have

$$\lim_{N, V \rightarrow \infty} (\Lambda_1/N) = \frac{1}{2}\rho \int d\mathbf{r}_{12} \exp(-r_{12}^2) = \frac{1}{2}\rho\pi^{D/2} \quad (2.13)$$

$$\lim_{N, V \rightarrow \infty} (\Lambda_2/N) = \frac{1}{4}\rho \int d\mathbf{r}_{12} \exp(-2r_{12}^2) = \frac{1}{4}\rho(\pi/2)^{D/2}. \quad (2.14)$$

In each cumulant order l the Gaussian pair interactions generate integrals which (with infinite limits) can be performed by standard manipulations. The result is that the β series for the infinite system excess free energy per particle has the following form:

$$\beta f(\beta) \sim b_{12}(D)\rho_D\beta - \sum_{n=2}^{\infty} \left[\sum_{j=2}^n b_{nj}(D)\rho_D^{j-1} \right] (-\beta)^n \equiv - \sum_{n=1}^{\infty} B_n (-\beta)^n, \quad (2.15)$$

where we have introduced the quantity

$$\rho_D = \pi^{D/2}\rho. \quad (2.16)$$

The separate contributions to the b_{nj} are irreducible cluster integrals with products of pair interactions serving as integrands. Some of the simpler irreducible clusters are illustrated in Fig. 1 as linear graphs in which vertices represent particles and lines connecting those vertices represent Gaussian pair interactions. Expressions (2.13) and (2.14) provide the simplest irreducible clusters respectively, namely those having two vertices connected by one and by two lines. In the present context irreducibility implies that graphs are connected but have no articulation (cutting) points. The coefficient $b_{nj}(D)$ in Eq. (2.15) collects contributions from all irreducible clusters having n lines and j vertices.

In order to evaluate a given $b_{nj}(D)$ it is first necessary to create a catalog of distinct irreducible cluster graphs for the given n and j . For any one of those graphs G , the corresponding contribution to $b_{nj}\rho_D^{j-1}$ is

$$I(G) = \frac{\rho_D^{j-1}}{\sigma(G)} \int d\mathbf{r}_{12} \cdots \int d\mathbf{r}_{1n} \prod_{(G)} \exp(-r_{ij}^2). \quad (2.17)$$

$1/\sigma(G)$ is a symmetry factor; it equals the number of distinguishable ways that the graph could be drawn between labelled vertices, divided by $n!$ and by a product of $k_{ij}!$, where k_{ij} is the number of direct interaction bonds between vertices i and j . After diagonalizing the quadratic form in (2.17) the integral can be evaluated in closed form with a result that always has the structure:

$$I(G) = \rho_D^{j-1} / \{ \sigma(G) [\tau(G)]^{D/2} \}, \quad (2.18)$$

where $\tau(G)$ is a positive integer characteristic of G .

The entire set of irreducible graphs with $n \leq 8$ has been catalogued and the corresponding contributions (2.18) have been evaluated. The resulting $b_{nj}(D)$ are shown in Table I, which also provides the numbers of contributing cluster species for each $b_{nj}(D)$. These results were obtained manually. It is conceivable that the procedure could be automated via computer, with higher order graphs both generated and evaluated to extend substantially the present tabulation.

III. SERIES NUMERICAL PROPERTIES

In order to examine the convergence properties of the β series (2.15) it is useful to examine the ratios

$$r_n = B_n(D, \rho_D) / B_{n-1}(D, \rho_D). \quad (3.1)$$

The ratio test for series⁴ specifies how these quantities (always positive in the present case) can reveal the radius of convergence R of the series. Specifically

$$\limsup_{n \rightarrow \infty} r_n = 1/R \quad (3.2)$$

if the limit exists.

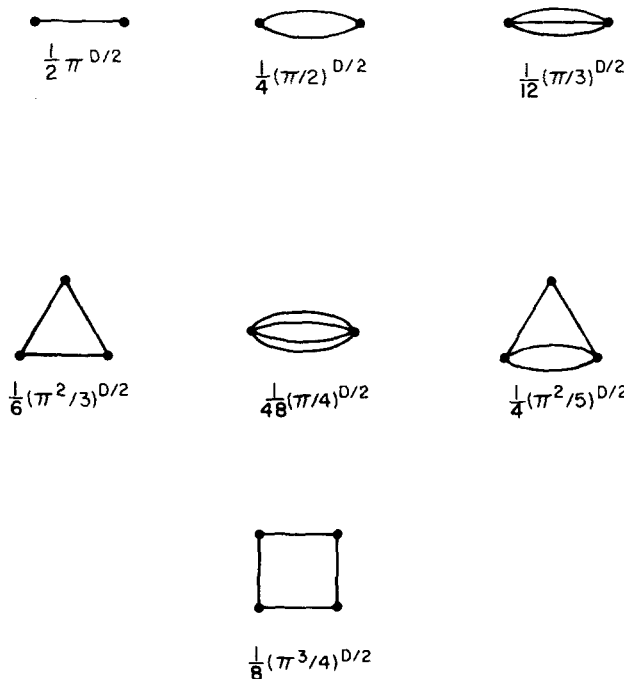


FIG. 1. Low-order irreducible clusters. Under the graph of each cluster species G is given the value of $I(G)$ [Eq. (2.17)], the corresponding contribution to $\beta f(\beta)$.

TABLE I. High-temperature series coefficients for the Gaussian core model excess free energy.

n, j	Cluster species	$b_{nj}(D)$
1, 2	1	$\frac{1}{2}$
2, 2	1	$\frac{1}{4}(2^{-D/2})$
3, 2	1	$\frac{1}{12}(3^{-D/2})$
3, 3	1	$\frac{1}{6}(3^{-D/2})$
4, 2	1	$\frac{1}{48}(4^{-D/2})$
4, 3	1	$\frac{1}{4}(5^{-D/2})$
4, 4	1	$\frac{1}{8}(4^{-D/2})$
5, 2	1	$\frac{1}{240}(5^{-D/2})$
5, 3	2	$\frac{1}{12}(7^{-D/2}) + \frac{1}{8}(8^{-D/2})$
5, 4	2	$\frac{1}{4}(7^{-D/2}) + \frac{1}{4}(8^{-D/2})$
5, 5	1	$\frac{1}{10}(5^{-D/2})$
6, 2	1	$\frac{1}{1440}(6^{-D/2})$
6, 3	3	$\frac{1}{48}(9^{-D/2}) + \frac{1}{12}(11^{-D/2}) + \frac{1}{48}(12^{-D/2})$
6, 4	6	$\frac{1}{12}(10^{-D/2}) + \frac{5}{16}(12^{-D/2}) + \frac{1}{2}(13^{-D/2}) + \frac{1}{24}(16^{-D/2})$
6, 5	3	$\frac{1}{4}(9^{-D/2}) + \frac{1}{2}(11^{-D/2}) + \frac{1}{12}(12^{-D/2})$
6, 6	1	$\frac{1}{12}(6^{-D/2})$
7, 2	1	$\frac{1}{10080}(7^{-D/2})$
7, 3	4	$\frac{1}{240}(11^{-D/2}) + \frac{1}{48}(14^{-D/2}) + \frac{1}{72}(15^{-D/2}) + \frac{1}{48}(16^{-D/2})$
7, 4	11	$\frac{1}{48}(13^{-D/2}) + \frac{1}{24}(16^{-D/2}) + \frac{1}{8}(17^{-D/2}) + \frac{1}{8}(18^{-D/2}) + \frac{1}{4}(19^{-D/2}) + \frac{3}{16}(20^{-D/2}) + \frac{1}{4}(21^{-D/2}) + \frac{1}{8}(24^{-D/2})$
7, 5	11	$\frac{1}{12}(13^{-D/2}) + \frac{1}{4}(16^{-D/2}) + \frac{1}{4}(17^{-D/2}) + \frac{1}{2}(18^{-D/2}) + \frac{3}{4}(19^{-D/2}) + \frac{1}{3}(20^{-D/2}) + \frac{1}{2}(21^{-D/2}) + \frac{1}{4}(24^{-D/2})$
7, 6	4	$\frac{1}{4}(11^{-D/2}) + \frac{1}{2}(14^{-D/2}) + \frac{1}{4}(15^{-D/2}) + \frac{1}{4}(16^{-D/2})$
7, 7	1	$\frac{1}{14}(7^{-D/2})$
8, 2	1	$\frac{1}{80640}(8^{-D/2})$
8, 3	5	$\frac{1}{1440}(13^{-D/2}) + \frac{1}{240}(17^{-D/2}) + \frac{1}{144}(19^{-D/2}) + \frac{1}{192}(20^{-D/2}) + \frac{1}{144}(21^{-D/2})$
8, 4	22	$\frac{1}{240}(16^{-D/2}) + \frac{1}{96}(20^{-D/2}) + \frac{1}{32}(22^{-D/2}) + \frac{1}{24}(23^{-D/2}) + \frac{1}{48}(24^{-D/2}) + \frac{1}{12}(25^{-D/2}) + \frac{1}{12}(26^{-D/2}) + \frac{1}{12}(27^{-D/2})$ $+ \frac{1}{8}(28^{-D/2}) + \frac{1}{6}(29^{-D/2}) + \frac{1}{8}(30^{-D/2}) + \frac{87}{384}(32^{-D/2}) + \frac{1}{8}(35^{-D/2}) + \frac{1}{32}(36^{-D/2})$
8, 5	33	$\frac{1}{48}(17^{-D/2}) + \frac{1}{4}(23^{-D/2}) + \frac{1}{6}(25^{-D/2}) + \frac{1}{2}(27^{-D/2}) + \frac{3}{8}(28^{-D/2}) + \frac{3}{8}(29^{-D/2}) + \frac{5}{4}(31^{-D/2}) + \frac{11}{16}(32^{-D/2})$ $+ \frac{1}{2}(33^{-D/2}) + 34^{-D/2} + \frac{1}{6}(36^{-D/2}) + \frac{1}{2}(37^{-D/2}) + \frac{1}{2}(40^{-D/2}) + \frac{1}{8}(45^{-D/2})$
8, 6	23	$\frac{1}{12}(16^{-D/2}) + \frac{5}{16}(20^{-D/2}) + \frac{1}{4}(22^{-D/2}) + \frac{1}{2}(23^{-D/2}) + \frac{1}{8}(24^{-D/2}) + 25^{-D/2} + \frac{3}{4}(26^{-D/2}) + \frac{1}{2}(27^{-D/2})$ $+ \frac{5}{8}(28^{-D/2}) + 29^{-D/2} + \frac{3}{4}(30^{-D/2}) + \frac{37}{48}(32^{-D/2}) + \frac{1}{2}(35^{-D/2}) + \frac{1}{8}(36^{-D/2})$
8, 7	5	$\frac{1}{4}(13^{-D/2}) + \frac{1}{2}(17^{-D/2}) + \frac{1}{2}(19^{-D/2}) + \frac{1}{4}(20^{-D/2}) + \frac{1}{4}(21^{-D/2})$
8, 8	1	$\frac{1}{16}(8^{-D/2})$

Figure 2 displays computed r_n values plotted versus n for $D=3$, $\rho_D=1$. The points show smooth behavior and suggest that as $n \rightarrow \infty$,

$$r_n \sim A_1 n + A_0 + A_{-1} n^{-1} + O(n^{-2}). \quad (3.3)$$

Similar results obtain for different ρ_D and D choices. Such asymptotic linearity of the r_n with n implies that $R=0$, and it was for this reason that the infinite-system-limit series shown in Eq. (2.15) was indicated to be asymptotic to $\beta f(\beta)$.

The vanishing of R seems to have a clear source. Negative real values of β with the positive Gaussian potentials (2.1) is a case equivalent to that with positive

real β and negative Gaussian potentials. This latter situation obviously involves instability with respect to collapse of the many-particle system into a molecular analog of a "black hole," with the positions of all particles virtually coincident. This collapse singularity at $\beta=0$ has no direct bearing on the melting and freezing phenomena for positive real β . It is only a mathematical annoyance which fortunately can be dealt with by the method presented in the following section.

Not only do the B_n appear to manifest smooth behavior with n , but so too do the component quantities $b_{nj} \rho_D^{j-1}$ when j is varied at fixed n . Figure 3 illustrates this point with a plot of the quantities $b_{8j} \rho_D^{j-1}$ for $D=3$, ρ_D

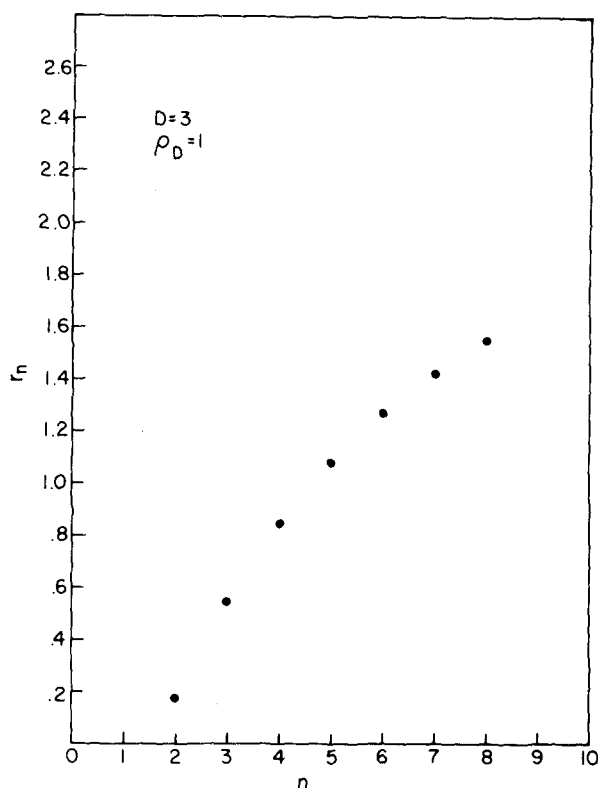


FIG. 2. Series coefficient ratios r_n [Eq. (3.1)] vs order n . For the case shown $D=3$ and $\rho_D=1$.

$=1$. The histogram shown conveys the clear impression of a discrete representation for a unimodal distribution. The corresponding plots for $n < 8$ have the same general appearance. Varying ρ_D at fixed $D=3$ and n has the effect of shifting the distribution horizontally while maintaining its unimodal character: increasing ρ_D shifts to larger j , decreasing ρ_D shifts to smaller j .

For $n > 2$, j spans the range from 2 up to n , inclusive. At the lower extreme two particle vertices in the relevant irreducible cluster are connected by n parallel lines ("watermelon" diagram) while at the upper extreme n vertices are linked by n lines in a polygon (" n -cycle" diagram). Between these extremes the value of j controls the average number of connections per vertex. Although there is no obvious reason why contributions to the free energy series should vary smoothly with this topological characteristic, this is nevertheless the case. It appears that deep mathematical reasons are yet to be discovered for this observation.

On account of the elementary way that dimension D enters the free energy series (see Table I) it is easy to study the way that the available series coefficients and their component parts depend on this parameter. Conventionally statistical mechanics has concerned itself with models embedded in Euclidean spaces, with $D=1, 2, 3, \dots$. However an axiomatic basis exists for the mathematical theory of spaces with noninteger D , and the statistical mechanics of many-particle aggregates in these spaces has legitimate meaning.⁵

Upon increasing D an interesting and perhaps unex-

pected feature occurs. The unimodal behavior previously illustrated for $b_{nj}\rho_D^{j-1}$ vs j can become bimodal. This is shown in Fig. 4 for $n=8$, $D=15$, $\rho_D=0.241506$. The phenomenon first appears for $n=8$ when $D \cong 13$ and becomes more and more pronounced as D increases. Its origin is clear from Table I. The midrange j values (for given n) have cluster contributions with larger integers raised to the $-D/2$ power than do the cluster contributions for extreme j values. Consequently choosing D to be large and positive will exert a discriminatory quenching effect on this midrange.

The tendency toward bimodality as D increases places increasing weight on clusters whose graphs are watermelon-like or cycle-like. This suggests that the statistical theory undergoes important simplifications in the $D \rightarrow \infty$ limit, at least for the high-temperature fluid phase.

IV. BOREL TRANSFORM

If Eq. (3.3) provides an accurate representation of the ratios defined in Eq. (3.1), then we can easily infer the asymptotic behavior of the B_n for large n . Specifically,

$$\ln B_n = C_0 + \sum_{k=m}^n \ln(Ak + A_0 + \dots), \quad (4.1)$$

where $m < n$ and C_0 is a suitable constant. This can be rewritten as follows:

$$\ln B_n = C_1 + n \ln A_1$$

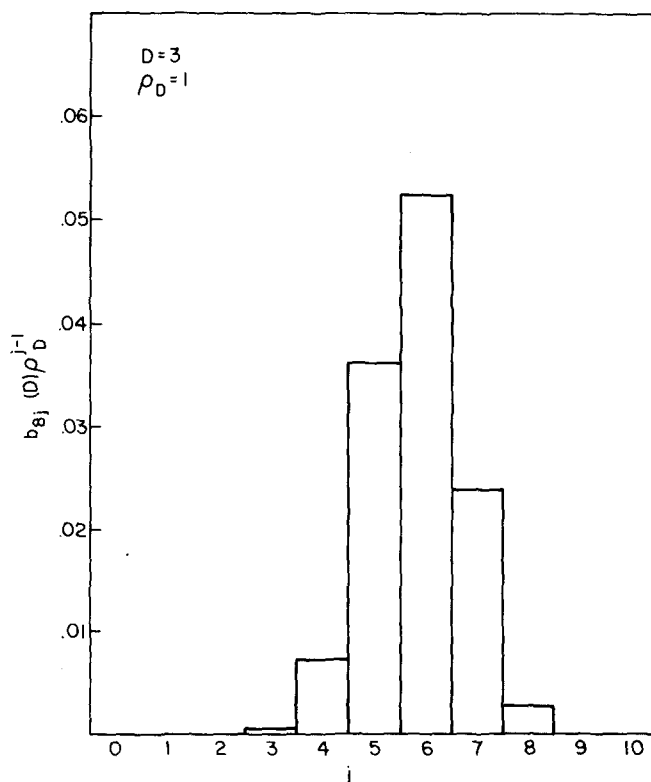


FIG. 3. Eighth-order cluster contributions $b_{8j}(D)\rho_D^{j-1}$ plotted vs j , the number of vertices. For the case shown $D=3$ and $\rho_D=1$.

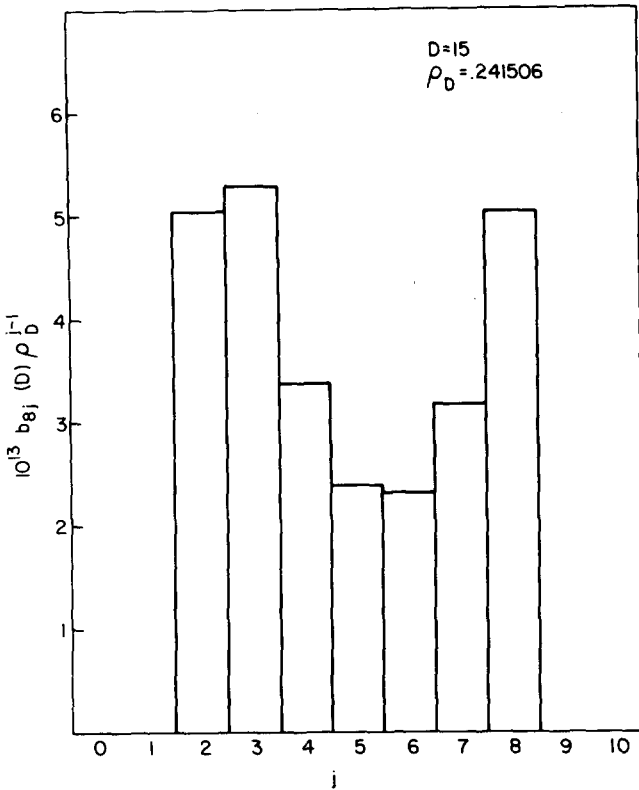


FIG. 4. Eighth-order cluster contributions vs j , for $D = 15$, $\rho_D = 0.241506$.

$$+ \sum_{k=m}^n \left[\ln k + \ln \left(1 + \frac{A_0}{A_1 k} + \dots \right) \right]. \quad (4.2)$$

If m and n are sufficiently large, the last logarithm in Eq. (4.2) may be replaced simply by $A_0/(A_1 k)$, and furthermore the sum may be replaced by an integral over k :

$$\begin{aligned} \ln B_n &\sim C_1 + n \ln A_1 + \int_{m-1/2}^{n+1/2} \left[\ln k + \frac{A_0}{A_1 k} \right] dk \\ &= C_2 + n \ln A_1 + \left(n + \frac{A_0}{A_1} + \frac{1}{2} \right) \ln \left(n + \frac{1}{2} \right) \\ &\sim C_3 + \left(\frac{A_0}{A_1} + \frac{1}{2} \right) \ln n + n \ln A_1 + n \ln n. \end{aligned} \quad (4.3)$$

With due regard for Stirling's factorial formula, this last expression is seen to be equivalent to:

$$B_n \sim K n^{\rho_0} \exp(\alpha n) n!, \quad (4.4)$$

where

$$\rho_0 = A_0/A_1, \quad \alpha = 1 + \ln A_1, \quad (4.5)$$

and K is a positive constant.

Asymptotic series coefficients have previously been observed to show behavior of type (4.4), in particular for the n -vector model in three dimensions.⁶ Just as in that former case, we too can employ the Borel transform to effect a formal summation of our divergent free energy series.

Set

$$\beta f(\beta) = \int_0^\infty \exp(-t) F(\beta t) dt; \quad (4.6)$$

F is the Borel transform of βf . It is easy to see that F must have the following series expansion:

$$F(x) = - \sum_{n=1}^\infty (B_n/n!) (-x)^n \quad (4.7)$$

to agree with Eq. (2.15). From Eq. (4.4) we see (via the ratio test) that the radius of convergence of the F series is

$$R_F = \exp(-\alpha) > 0. \quad (4.8)$$

Therefore $F(x)$ is analytic in the neighborhood of $x=0$.

In Appendix A it is shown that $F(x)$ possesses a branch point singularity at

$$x = - \exp(-\alpha) \quad (4.9)$$

with the following leading-order character:

$$-K\Gamma(\rho_0 + 1) [1 + x \exp(\alpha)]^{-\rho_0 - 1}. \quad (4.10)$$

This requires a branch cut from the position indicated in (4.9) along the negative axis. Evidently this singularity is the principal manifestation of the collapse phenomenon already discussed.

When $D=1$ no phase transition can occur.⁷ The free energy must vary smoothly along the positive β axis, and in fact it must be analytic for $0 < \beta < +\infty$. For very large positive β the repelling Gaussian particles will have nevertheless continuously settled into a regular array with nearly equal spacing between neighbors. Any residual motions in this regular array can be described by harmonic normal modes. It is then elementary to show that for $D=1$

$$\beta f(\beta) \sim \beta \phi + \frac{1}{2} \ln \beta + O(1), \quad (\beta \rightarrow +\infty) \quad (4.11)$$

where ϕ is the potential energy per particle in the periodic linear array. In order to yield this low temperature free energy, the Borel transform for $D=1$ must obey the following:

$$F(x) \sim \phi x + \frac{1}{2} \ln x + \dots, \quad (x \rightarrow +\infty). \quad (4.12)$$

In contrast to the relatively simple (and uninteresting) one-dimensional case, we expect that when $D=2, 3, 4, \dots$, $\beta f(\beta)$ will have a singularity on the positive real axis, specifically at the thermodynamic freezing point $\beta = \beta_f$. This singularity is associated with "hetero-phase" fluctuations⁸⁻¹¹ that constitute microscopic crystallites in the stable fluid phase. We shall examine this phenomenon at greater length in the following Sec. V, but for the moment we accept its validity and note that in order to have a singularity at β_f , $F(x)$ must be exponentially increasing as $x \rightarrow +\infty$:

$$F(x) \sim \exp(x/\beta_f) M(x). \quad (4.13)$$

M is a modulation factor that is dominated at infinity by the exponential factor. In principle the convergent power series (4.7) for F contains information sufficient to determine the freezing point β_f through (4.13).

At least while D is equal to 2, 3, 4, . . . , there is no analytic continuation that can be expected to supply the crystal-phase free energy, starting from the Borel transform (4.6) that is the appropriate representation for the infinite-system high-temperature fluid phase.

V. CRYSTALLITE DISTRIBUTION

We now turn attention to the geometry of particle arrangement. In particular we seek to identify regions within the stable fluid in which crystalline order locally obtains. These microscopic crystallites could serve as nucleation sites for growth of a macroscopic solid phase if the temperature were lowered below the thermodynamic freezing point. As we shall see, the size distribution of crystallites is intimately related to the Borel transform introduced in Sec. IV.

We assume that the structure of the low-temperature crystal is known at the density of interest.¹ In particular this knowledge includes geometric details about the positions (i. e., distances and relative angles) of particles in successive coordination shells about a given particle.

We now introduce a criterion for crystallinity through a function $C_1(i)$ which is unity if particle i is "properly coordinated," but is zero otherwise. Obviously $C_1(i)$ is a function of all particle positions in the system, not just the position of i . For present purposes the precise form of $C_1(i)$ is not relevant, and indeed some freedom of choice exists in its selection. However we have in mind that in order to equal 1 this function will require correct crystalline order in the first (and possibly the first two or three) coordination shells, within reasonable distance and angle limits of the ideal $T=0$ crystal structure. Within the stable fluid phase only a small fraction of the particles at any instant will be properly coordinated, while in the low-temperature crystal all will, with the possible exception of a few associated with defects.

Further discussion of crystallites is facilitated by use of the grand ensemble. Let

$$N_C(\mathbf{r}_1 \cdots \mathbf{r}_N) = \sum_{i=1}^N C_1(i) \quad (5.1)$$

represent the number of properly coordinated particles when the system contains precisely N particles at the indicated positions. Then

$$\langle N_C \rangle = Z_G^{-1} \sum_{N=0}^{\infty} (y^N / N!) \int d\mathbf{r}_1 \cdots \int d\mathbf{r}_N N_C(\mathbf{r}_1 \cdots \mathbf{r}_N) \times \exp[-\beta\Phi(\mathbf{r}_1 \cdots \mathbf{r}_N)] \quad (5.2)$$

gives the mean value of N_C in the grand ensemble, where Z_G is the grand partition function:

$$Z_G = \sum_{N=0}^{\infty} (y^N / N!) \int d\mathbf{r}_1 \cdots \int d\mathbf{r}_N \exp[-\beta\Phi_N(\mathbf{r}_1 \cdots \mathbf{r}_N)] \quad (5.3)$$

and y is the fugacity:

$$y = \exp(\beta\mu) / \lambda^D. \quad (5.4)$$

In order to discuss the aggregation of properly coordinated

particles into crystallites it is necessary to introduce a two-particle criterion, which will be expressed by the function $C_2(i, j)$. This new function will be unity if (a) both particles i and j are properly coordinated, and (b) i and j serve as nearest neighbors to one another; otherwise it will vanish. Obviously C_2 is symmetric:

$$C_2(i, j) = C_2(j, i). \quad (5.5)$$

The crystalline coordination criteria expressed by C_1 and C_2 naturally partition the properly coordinated particles into mutually exclusive subsets. A subset (crystallite) containing just one particle i will preclude the existence of some other particle j for which $C_2(i, j) = 1$. However subsets (crystallites) with $l > 1$ particles are such that any pair i, j are connected either directly by a C_2 relation, or indirectly by a chain of C_2 relations involving intermediate particles in the same subset (crystallite). Hence

$$N_c = \sum_{l=1}^{\infty} l n_l, \quad (5.6)$$

where n_l is the number of l -particle crystallites.

The procedure for identifying crystallites parallels that which has been used to identify physical clusters (droplets) in the vapor phase.¹² Therefore it is possible to adapt the formal techniques for studying the distribution of physical clusters in the grand ensemble to the study of crystallite distribution. This allows an exact expression for $\langle n_l \rangle$ to be written down directly:

$$\langle n_l \rangle = (y^s / s!) \int_{(l)} d\mathbf{r}_1 \cdots \int d\mathbf{r}_l \exp[-\beta(\Phi_l + W_l)]. \quad (5.7)$$

Here the Dl -dimensional integration region denoted by (l) constrains the l particles to those relative configurations which are consistent with the existence of the l crystallite. W_l is a cavity free energy representing the amount of reversible isothermal work necessary to rearrange the medium in such a way that it can accommodate the given l crystallite. This quantity can be expressed as a ratio of grand partition functions, with and without the interactions entailed by the presence of an l crystallite:

$$\exp[-\beta W_l(\mathbf{r}_1 \cdots \mathbf{r}_l, \beta, y)] = Z_G^{-1} \sum_{N=0}^{\infty} (y^N / N!) \int_{(l, N)} d\mathbf{r}_{l+1} \cdots \int d\mathbf{r}_{l+N} \times \exp\{-\beta[\Phi_N(\mathbf{r}_{l+1} \cdots \mathbf{r}_{l+N}) + \Phi_{l, N}(\mathbf{r}_1 \cdots \mathbf{r}_l | \mathbf{r}_{l+1} \cdots \mathbf{r}_{l+N})]\}. \quad (5.8)$$

Notice that the configuration integrals explicitly shown here contain interactions both within the set of N medium particles (Φ_N) as well as cross interactions between crystallite particles and medium particles ($\Phi_{l, N}$). Configurations allowed by the integration region (l, N) are those with $\mathbf{r}_{l+1} \cdots \mathbf{r}_{l+N}$ anywhere in system volume V except those which would violate the existence of the fixed l crystallite.

For large l we can reasonably expect that the crystallite occurrence probability will be determined by macroscopic attributes. In particular we would expect to find in the fluid

$$\langle n_i \rangle / V \sim \exp[-k_0 l - k_1 l^{(D-1)/D} - o(l^{(D-1)/D})] . \quad (5.9)$$

The leading terms shown, respectively, represent the bulk free energy difference between the (thermodynamically unstable) crystal phase and the (thermodynamically stable) fluid, and a positive interfacial free energy between crystal and fluid. At temperatures just above the freezing point and at fixed overall density we will have

$$k_0 = K_0 \Delta \beta + 0[(\Delta \beta)^2] , \quad (5.10)$$

$$\Delta \beta = \beta_f - \beta , \quad K_0 > 0$$

while k_1 remains positive when $\Delta \beta \rightarrow 0$:

$$k_1 = K_1 + 0(\Delta \beta) , \quad K_1 > 0 . \quad (5.11)$$

On account of their anomalous structure in comparison with the fluid overall, the crystallites represent regions of anomalous interaction energy. This energy will contain both bulk and surface contributions. For large l we expect the anomalous energy contribution to the fluid to have the form

$$E_1 = [e_0 l + e_1 l^{(D-1)/D} + \dots] \langle n_i \rangle$$

$$\sim V \exp[-k_0 l - k_1 l^{(D-1)/D} + \dots] . \quad (5.12)$$

Evidently the two leading terms in the exponential will be the same as for $\langle n_i \rangle$ alone. The total anomalous energy that can be attributed to all crystallites obviously will be

$$E_{cr} = \sum_{i=1}^{\infty} E_i . \quad (5.13)$$

In the neighborhood of the freezing point this gives

$$E_{cr} \cong V \sum_{i=1}^{\infty} \exp[-K_0 \Delta \beta l - K_1 l^{(D-1)/D} + \dots] , \quad (5.14)$$

which has an essential singularity at the origin of the complex $\Delta \beta$ plane.

The excess thermodynamic energy E_{ex} is related to the previously introduced excess Helmholtz free energy per particle f by

$$E_{ex} = \langle N \rangle (\partial \beta f / \partial \beta)_{V, \langle N \rangle} . \quad (5.15)$$

The singular portion of E_{ex} shown in Eq. (5.14) must have a progenitor in f , of course. Thus we can conclude that βf also includes an essentially singular part, arising from crystallites in the fluid, that is adequately represented by the following expression:

$$\beta f_{cr}(\beta) = \sum_{i=1}^{\infty} \exp[-K_0 \Delta \beta l - K_1 l^{(D-1)/D} + \dots] . \quad (5.16)$$

Here we have recognized that the differentiation required by Eq. (5.15), as well as its inverse, will not affect the two leading exponential terms shown.

Upon making the replacement

$$l = t / (K_0 \beta_f) \quad (5.17)$$

in Eq. (5.16), followed by replacement of the sum by an integral (this will not affect the leading order singularity of interest), we obtain

$$\beta f_{cr}(\beta) = \int_0^{\infty} \exp(-t) F_{cr}(\beta t) dt , \quad (5.18)$$

wherein

$$F_{cr}(x) = \exp[x/\beta_f - K_1 (K_0 \beta_f^2)^{(1-D)/D} x^{(D-1)/D} + \dots] . \quad (5.19)$$

The important point to notice is that (5.18) has the form of a Borel transform.

The singular function f_{cr} constitutes only part of f :

$$f(\beta) = f_{cr}(\beta) + f_a(\beta) ; \quad (5.20)$$

the remainder f_a is analytic at β_f . The Borel transform $F_a(x)$ of f_a then cannot increase exponentially as $x \rightarrow +\infty$. We can write

$$\beta f(\beta) = \int_0^{\infty} \exp(-t) [F_{cr}(\beta t) + F_a(\beta t)] dt . \quad (5.21)$$

Borel transforms are equivalent to Laplace transforms by trivial change of variables, and on account of the uniqueness of the latter we can infer that

$$F(x) = F_{cr}(x) + F_a(x) , \quad (5.22)$$

where F is the function originally introduced in Eq. (4.6). Referring to Eq. (5.19), we see that $F(x)$ has the following large- x behavior:

$$F(x) \sim \exp[x/\beta_f - K_1 (K_0 \beta_f^2)^{(1-D)/D} x^{(D-1)/D} + \dots] . \quad (5.23)$$

It is this conclusion which underlies the earlier Eq. (4.13).

The result (5.23) shows that the existence and properties of crystallites are encoded in the β series for free energy, and that the Borel transform is required to decode that information. The relation between the specific irreducible clusters of the β series on the one hand, and the physical crystallite clusters on the other hand, is obscure. In particular it is not clear whether any topologically distinctive subset of the irreducible clusters dominates the singular behavior in $f_{cr}(\beta)$. The advantage of the Gaussian core model is that since exact β series coefficients of any finite order can in principle be obtained, this topological question need not be answered.

VI. METASTABLE EXTENSIONS

While the singular free energy f_{cr} has a fundamental significance in phase transition theory, its numerical contribution to fluid phase properties is no doubt very small. In fact most pure fluids can readily be supercooled below their thermodynamic freezing points, and molecular dynamics simulation shows that the Gaussian core model is no exception.² The question then arises whether the present formalism lends itself gracefully to the description of the supercooled fluid. The answer appears to be affirmative.

Evidently all that is required to generate a metastable extension of the fluid free energy is to subtract the exponentially increasing part from the Borel transform F . This can be done by subtracting F_{cr} to leave F_a , as indicated earlier in Eq. (5.22). But in fact the subtraction is not unique; there exists an infinite set of functions which qualify. If F_{∞} is any one of these the corresponding free energy with metastable extension $f_{m\infty}$ will be:

$$\beta f_{\text{me}}(\beta) = \int_0^{\infty} \exp(-t) [F(\beta t) - F_{\infty}(\beta t)] dt. \quad (6.1)$$

One must ensure that each function F_{∞} is analytic at least within a circle about the origin including the point identified in Eq. (4.9), so as to leave unmodified the collapse singularity of the free energy at $\beta = 0$.

All of the qualifying subtraction functions F_{∞} share with F_{cr} a common asymptotic behavior as $x \rightarrow +\infty$. However they can differ widely in their behavior around $x = 0$. In particular we could choose a function $F_{\infty}(x)$ whose power series coefficients up to some preselected order (say l_0) identically vanished. Under this circumstance βf_{me} in Eq. (6.1) would agree exactly with βf through $O(\beta^{l_0})$, and so the metastable extension procedure would only affect higher powers of β . If l_0 were chosen to be very large, Eq. (6.1) would presumably give an accurate approximation to the exact free energy over the entire stable fluid range, but upon entering the metastable regime the function βf_{me} is liable to exhibit unusual behavior indicative of partial crystallization into domains of size $\approx l_0$. Choosing l_0 to be very small would avoid that problem, but would render βf_{me} a poor free energy approximation over the stable fluid range.

Evidently an "intermediate" value of l_0 is required. Intuition suggests that the optimal choice should correspond to the critical nucleus size. According to standard nucleation theory¹³ this size (a) depends on the time scale of the experiment by which metastable states are prepared and observed, and (b) for typical laboratory conditions will occur in the range of $l_0 \approx 10^2$. In any case it is fitting that our subtractive procedure should be able to reflect the kinetics of phase change.

These considerations bear on the connection between the β series for thermodynamic properties derived in this paper and the molecular dynamics results for the Gaussian core model. The basic problem is to assemble the available series coefficients (Table I) in a form which will logically and accurately represent the simulation data, including its metastable regime. Since the critical nucleus size l_0 will normally exceed the highest order to which the β series will have been evaluated, the spirit of the subtractive procedure can be implemented merely by constructing approximants to $F - F_{\infty}$ which agree with the exact β series as far as it is known, and which grow with increasing x less rapidly than exponentially. Having established [Eq. (4.10)] that the Borel transform contains algebraic branch points in the complex plane it seems natural to consider the following approximants:

$$F(x) - F_{\infty}(x) \approx Qx \prod_{j=1}^m (1 - x/x_j)^{q_j}, \quad (6.2)$$

where the constants Q , q_j , and x_j are selected to reproduce the available power series coefficients. It should be noted that the family of functions shown in Eq. (6.2) arises by constructing Padé rational approximants¹⁴ (with denominator order greater than numerator order) to the logarithmic derivative of $F - F_{\infty}$. The functions in Eq. (6.2) obviously will yield metastable extensions since they grow at most algebraically as $x \rightarrow +\infty$.

Appendix B shows a specific example of an approximant of type (6.2) for the Gaussian core model.

VII. DISCUSSION

Although the Borel transform offers a convenient way to handle the collapse singularity of the Gaussian core model, its use to study phase change has broader significance. The connection between this transform and the distribution of crystallites established in Sec. V transcends this specific model. For classical models with repelling pair interactions of the type:

$$v(r_{ij}) = \epsilon(\sigma/r_{ij})^n, \quad (7.1)$$

$$n > 3,$$

it can easily be shown that $\beta f(\beta)$ has a convergent power series expansion in the variable $\beta^{D/n}$. Consequently the analytical behavior near the origin is profoundly different from that of the Gaussian core model. Nevertheless these inverse-power potentials also produce freezing transitions so that the respective Borel transforms must display the asymptotic behavior shown in Eq. (5.23).

It is desirable to extend the present study in a way which includes attractive intermolecular forces outside the repelling core region. This can be done simply with a two-Gaussian pair interaction, and in fact a rather accurate fit to the minimum region of noble gas potentials is possible this way. Although the computations become somewhat more complex, it is still possible to evaluate β series coefficients exactly, due once again to the special nature of Gaussians. With attractive forces present both crystallization and vapor condensation can occur. It is clear that the role played by crystallites in the former is adopted by liquid droplets in the latter.¹² Consequently we expect that in the vapor condensation region of the phase plane the Borel transform would obey an asymptotic relation of type (5.23), but including parameters that are appropriate to bulk and surface properties of droplets. It is even possible that the liquid-vapor critical point may be amenable to study by our β series techniques.

An area of special concern is how small variations in the space dimension D away from the integer values 2, 3, 4, ..., will influence the crystallization process. There is reason to hope that the Gaussian core model will help to illuminate this difficult question.

APPENDIX A

We can extract the leading singularity (i. e., the one nearest the origin) in $F(x)$ from the associated function

$$S(x) = -K \sum_{n=1}^{\infty} n^{\beta_0} [-x \exp(\alpha)]^n. \quad (A1)$$

S and F have series coefficients with a common large- n form. Set

$$\exp(-y) = -x \exp(\alpha) \quad (A2)$$

so that

$$S = -K \sum_{n=1}^{\infty} n^{\beta_0} \exp(-ny). \quad (A3)$$

TABLE II. Values of $x_1(D, \rho_D)$ and $q_1(D, \rho_D)$ in Eq. (B1).

$\rho_D =$	0	0.25	0.50	1.0	2.0
$x_1(D=1)$	-214.27	-10.483	-5.3731	-2.7207	-1.3690
$q_1(D=1)$	-37.878	-1.8532	-0.94985	-0.48095	-0.24201
$x_1(D=2)$	-43.200	-10.2857	-5.8378	-3.1304	-1.6241
$q_1(D=2)$	-5.4000	-1.2857	-0.72973	-0.39130	-0.20301
$x_1(D=3)$	-30.699	-10.746	-6.5131	-3.6430	-1.9364
$q_1(D=3)$	-2.7135	-0.94985	-0.57568	-0.32200	-0.17115
$x_1(D=4)$	-27.574	-11.676	-7.4057	-4.2772	-2.3184
$q_1(D=4)$	-1.7234	-0.72973	-0.46286	-0.26733	-0.14490

If x is real and only slightly to the positive side of $-\exp(-\alpha)$ then y is real and positive, but small. In that event the sum in (A3) will be dominated by terms with large n , and these terms will vary sufficiently slowly with n that the sum may be replaced by an integral. Thus

$$\begin{aligned}
 S &\cong -K \int_0^\infty n^{\rho_0} \exp(-ny) dn \\
 &= -Ky^{-\rho_0-1} \int_0^\infty t^{\rho_0} \exp(-t) dt \\
 &= -K\Gamma(\rho_0 + 1)y^{-\rho_0-1}. \tag{A4}
 \end{aligned}$$

To the same order in which the preceding formula is valid we can write

$$y \cong 1 + x \exp(\alpha). \tag{A5}$$

Therefore when x is near to $-\exp(-\alpha)$,

$$S(x) \cong -K\Gamma(\rho_0 + 1)[1 + x \exp(\alpha)]^{-\rho_0-1}. \tag{A6}$$

This is the result upon which (4.10) in the text is based.

APPENDIX B

The simplest nontrivial approximant of the type shown in Eq. (6.2) corresponds to $m=1$, i.e., it is the case of a single branch point:

$$F(x) - F_\infty(x) = Qx(1 - x/x_1)^{q_1}. \tag{B1}$$

The three parameters Q , x_1 , and q_1 can be selected to cause the first three terms in the expansion of (B1),

$$\begin{aligned}
 F(x) - F_\infty(x) &= Qx - (Qq_1/x_1)x^2 \\
 &\quad + [\frac{1}{2}Qq_1(q_1 - 1)/x_1^2]x^3 - \dots \tag{B2}
 \end{aligned}$$

to reproduce the same three terms in the exact expansion for the Borel transform F :

$$F(x) = \frac{\rho_D x}{2} - \frac{\rho_D x^2}{8(2^{D/2})} + \frac{(\rho_D + 2\rho_D^2)x^3}{72(3^{D/2})} - \dots \tag{B3}$$

This requirement leads to the following expressions:

$$\begin{aligned}
 Q &= \rho_D/2, \\
 x_1 &= [\frac{1}{4}(\frac{1}{2})^{D/2} - \frac{2}{9}(\frac{2}{3})^{D/2} - \frac{4}{9}(\frac{2}{3})^{D/2}\rho_D]^{-1}, \tag{B4} \\
 q_1 &= [1 - \frac{8}{9}(\frac{4}{3})^{D/2} - \frac{16}{9}(\frac{4}{3})^{D/2}\rho_D]^{-1}.
 \end{aligned}$$

With this approximant the free energy (subject now to metastable extension below the freezing temperature) is represented thus:

$$\begin{aligned}
 \beta f_{me}(\beta) &= \frac{1}{2}\beta\rho_D \int_0^\infty dt t \\
 &\quad \times \exp(-t) \left[1 - \frac{\beta t}{x_1(D, \rho_D)}\right]^{q_1(D, \rho_D)}. \tag{B5}
 \end{aligned}$$

Table II presents some numerical values computed for x_1 and q_1 according to formulas (B4). It should be stressed that exact cluster information only through third order has been utilized at this level of approximation. With more accurate approximants of higher order we can expect some modification of the collapse singularity described by x_1 and q_1 in Eq. (B5).

¹F. H. Stillinger, *J. Chem. Phys.* **65**, 3968 (1976).
²F. H. Stillinger and T. A. Weber, *J. Chem. Phys.* **68**, 3837 (1978); Erratum, *ibid.* **70**, 1074E (1979).
³H. Cramér, *Mathematical Methods of Statistics* (Princeton University, Princeton, 1946), Chap. 15.
⁴R. C. Buck, *Advanced Calculus*, 2nd ed. (McGraw-Hill, New York, 1965), p. 161.
⁵F. H. Stillinger, *J. Math. Phys.* **18**, 1224 (1977).
⁶J. C. LeGuillou and J. Zinn-Justin, *Phys. Rev. Lett.* **39**, 95 (1977).
⁷D. Ruelle, *Statistical Mechanics* (Benjamin, New York, 1969), p. 134.
⁸A. F. Andreev, *Soviet Physics JETP* **18**, 1415 (1964).
⁹M. E. Fisher, *Physics* **3**, 255 (1967).
¹⁰W. Klein, D. J. Wallace, and R. K. P. Zia, *Phys. Rev. Lett.* **37**, 639 (1976).
¹¹V. Ya. Krivnov, B. N. Provotorov, and V. L. Éidus, *Theor. Math. Phys.* **26**, 238 (1976).
¹²F. H. Stillinger, *J. Chem. Phys.* **38**, 1486 (1963).
¹³A. Van Hook, *Crystallization* (Reinhold, New York, 1961).
¹⁴G. A. Baker, *Essentials of Padé Approximants* (Academic, New York, 1975).